

## Magnetic and Orbital Ordering of $\text{KCuF}_3$ Studied by Resonant X-ray Scattering

Chia Hung Lai<sup>a</sup>, Wen-Bin Wu<sup>b</sup>, Chi Liang Huang<sup>c</sup>, Youichi Murakami<sup>d</sup>, Jun Okamoto<sup>b</sup>,  
and Di-Jing Huang<sup>b</sup>

<sup>a</sup>National Tsing Hua Univ., <sup>b</sup>NSRRC, <sup>c</sup>Tamkang Univ., <sup>d</sup>KEK CMRC/PF

### Abstract

We have studied the magnetic and orbital orderings in Cu  $3d$  orbitals of  $\text{KCuF}_3$  by using Cu K-edge resonant X-ray scattering. For the orbital reflection (1 0 5) at quadrupole transition, however, no clear transition was observed about 40 K. This shows that the coupling between spins and orbitals in Cu  $3d$  orbitals is small in *type-a* orbital ordering of  $\text{KCuF}_3$ .

**Keywords:** orbital ordering, resonant X-ray scattering, polarization analysis

### Background and Purpose

One of the hot subjects in the research of strongly correlated electron systems is the interplay between charge, orbital and spin degrees of freedoms. The magnetic and orbital properties of the pseudocubic perovskite  $\text{KCuF}_3$  have been studied in the past half century [1-6]. The charge-transfer insulator  $\text{KCuF}_3$  is an archetype of orbital ordered material with large exchange interaction energy.  $\text{KCuF}_3$  has been known to show one-dimensional quantum antiferromagnetic properties along  $c$  axis originating from the super-exchange interaction between the  $e_g$  orbitals of  $\text{Cu}^{2+}$ . Because of the Jahn-Teller distortion in the tetragonal structure, the degeneracy of the two  $e_g$  orbitals forms a pattern of orbital ordering. There are two mechanisms of orbital ordering [7,8]; First, electron-phonon coupling gives rise to Jahn-Teller distortion and then produces orbital ordering. Second, the super-exchange interaction leads to orbital ordering and then produces Jahn-Teller distortion. In the second one, orbital ordering can be enhanced by the presence of magnetic ordering. Therefore, the study of relations between magnetic and orbital orderings has been interested.

Figure 1 illustrates the two-different stacking of orbital orderings of  $\text{KCuF}_3$ . They form two types of antiferromagnetic structures (*type-a* and *type-d*) in  $\text{KCuF}_3$ . Neel temperature of these two structures are  $38 \pm 1$  K and  $22 \pm 4$  K for *type-a* and *type-d*, respectively [1].

Several resonant hard X-ray scattering (RXS) measurements have been done at the Cu K-edge to study the magnetic and orbital orderings in the Cu orbitals. For magnetic ordering, RXS peak appears below Neel temperature of 38 K and increases its intensity as temperature decreases. As for orbital ordering, its RXS peak intensity is constant down to 43 K but increases below this temperature and saturates below Neel temperature [2,3]. These observations show close relationship between magnetic and orbital orderings at low temperature, such as two-stage orbital ordering [9]. But in these RXS measurements, magnetic orderings show finite RXS intensities at the photon energies of both the electric dipole transition ( $1s \rightarrow 4p$ ) and the quadrupole transition ( $1s \rightarrow 3d$ ), but orbital orderings show finite RXS intensity only at the photon energies at the electric dipole transitions [2,3,10]. Orbital ordering in the Cu  $3d$  orbitals is reflected in the RXS orbital ordering peak observe at the Cu K-edge quadrupole transition, but it has not studied precisely yet.

We have so far studied magnetic ordering of  $\text{KCuF}_3$  in the Cu  $3d$  orbitals directly by using resonant soft X-ray scattering at the Cu  $L_3$ -edge [11]. As shown in Fig. 2, intensity of magnetic reflection at (0 0 1) increases below Neel temperature, which matches with reported Cu K-edge RXS data [2,3].

We have done Cu K-edge RXS measurement on the same sample with polarization analysis technique and tuned incident photon energy at the quadrupole transition to study the detail properties of magnetic and orbital orderings at the Cu  $3d$  orbitals in  $\text{KCuF}_3$ .

### Experimental Summary

$\text{KCuF}_3$  single crystal is prepared by Murakami Group at KEK; first  $\text{KCuF}_3$  poly crystals were grown by

aqueous solution precipitation method and then  $\text{KCuF}_3$  single crystal was fabricated from the poly crystals by the Bridgman method in an Ar atmosphere.  $\text{KCuF}_3$  single crystal is grown by controlling temperature gradient of the cell not by moving sample position in order to avoid the influence of motor vibration on sample quality. We did RXS measurement of *type-a*  $\text{KCuF}_3$  single crystal at the Cu K-edge at the BL12B2 beamline. Figure 3 shows the schematic representation of experimental setup. In order to suppress the intensity of charge reflection, we used  $\text{LiF}$  (0 0 4) as an analyzer crystal which satisfies the depolarize geometry condition at Cu K-edge. We choose the perovskite structure ( $a' = b' = 5.856 \text{ \AA}$ ,  $c' = 7.847 \text{ \AA}$ ) as a unit cell in our experiment. The two different stacking of orbital orderings in  $\text{KCuF}_3$  form two orbital reflections (1 0 5) for *type-a* and (1 0 4) for *type-d*.

### Results and Discussion

First we compared X-ray absorption spectroscopy (XAS) and diffraction anomalous fine structure (DAFS) of orbital ordering (1 0 5) for *type-a* at Cu K-edge. Figure 4(a) shows that the integrated intensity of the orbital ordering for *type-a* is enhanced drastically when the photon energy is tuned near the electric dipole transition ( $1s \rightarrow 4p$ ; 8995 eV), although it was less pronounced at the quadrupole transition ( $1s \rightarrow 3d$ ; 8980 eV) around the Cu K-edge. The DAFS line is consistent with the other data <sup>[2,3]</sup>, although measuring different orbital reflections.

We also compared the intensity of two orbital reflections (1 0 5) for *type-a* and (1 0 4) for *type-d* to examine the quality of  $\text{KCuF}_3$  setting incident photon energy at the Cu K-edge peak of 8995 eV. Figure 4 (b) represents the  $\sigma$ - $\pi'$  orbital diffraction intensities of *type-a* (1 0 5) and *type-d* (1 0 4) structures. We found that the intensity of orbital ordering from *type-d* was about 0.3 % of that from *type-a*. This observation suggests that our sample is a nearly pure *type-a* single crystal.

In order to study the coupling between magnetic and orbital orderings in Cu  $3d$  electronic structures, we have done RXS measurement of orbital ordering for *type-a* (1 0 5) by tuning photon energy at the quadrupole transition of Cu ( $1s \rightarrow 3d$ ) about 8980 eV. Figure 5 shows temperature dependence of scattering intensity at momentum transfer  $Q = (1\ 0\ 5)$  from 12 K to 60 K. No clear intensity drop was observed at magnetic transition temperature at 38 K, which was different from the reported data at dipole transition photon energy <sup>[2-3]</sup>. Our result shows that the coupling between spin and orbital degree of freedom in Cu  $3d$  electronic structures is small in *type-a* orbital ordering of  $\text{KCuF}_3$ .

### Challenges

Since Cu  $3d$   $e_g$  unoccupied states are narrow, we may need more precise check for selecting incident photon energies in the quadrupole transition.

### References

- [1] M. Ikebe, M. Date, *J. Phys. Soc. Jpn.* **30**, 93 (1971).
- [2] R. Caciuffo, L. Paolasini, A. Sollier, P. Ghigna, E. Pavarini, J. van den Brink, M. Altarelli, *Phys. Rev. B* **65**, 174425 (2002).
- [3] L. Paolasini, R. Caciuffo, A. Sollier, P. Ghigna, M. Altarelli, *Phys. Rev. Lett.* **88**, 106403 (2002).
- [4] M. Takahashi, M. Usuda, J. Igarashi, *Phys. Rev. B* **67**, 064425 (2003).
- [5] N. Binggeli, M. Altarelli, *Phys. Rev. B* **70**, 085117 (2004).
- [6] K. Ishii, S. Ishihara, Y. Murakami, K. Ikeuchi, K. Kuzushita, T. Inami, K. Ohwada, M. Yoshida, I. Jarrige, N. Tatami, S. Niioka, D. Bizen, Y. Ando, J. Mizuki, S. Maekawa, Y. Endoh, *Phys. Rev. B* **83**, 241101 (2011).
- [7] J. Kanamori, *J. of Appl. Phys.* **31**, S14 (1960).
- [8] K. I. Kugel, D. I. Khomskii, *Sov. Phys.-JETP* **37**, 725 (1974).
- [9] J. T. Lee, S. Yuan, S. Lal, Y. I. Joe, Y. Gan, S. Smadici, K. Finkelstein, Y. Feng, A. Rusydi, P. M. Goldbart, S. L. Cooper, P. Abbamonte, *Nat. Phys.* **8**, 63 (2012).
- [10] C. Mazzoli, L. Paolasini, F. de. Bergevin, P. Ghigna, R. Caciuffo, *Physica B* **378-380**, 563 (2006).
- [11] C. H. Lai, Ph. D thesis, National Tsing-Hua University (2014).

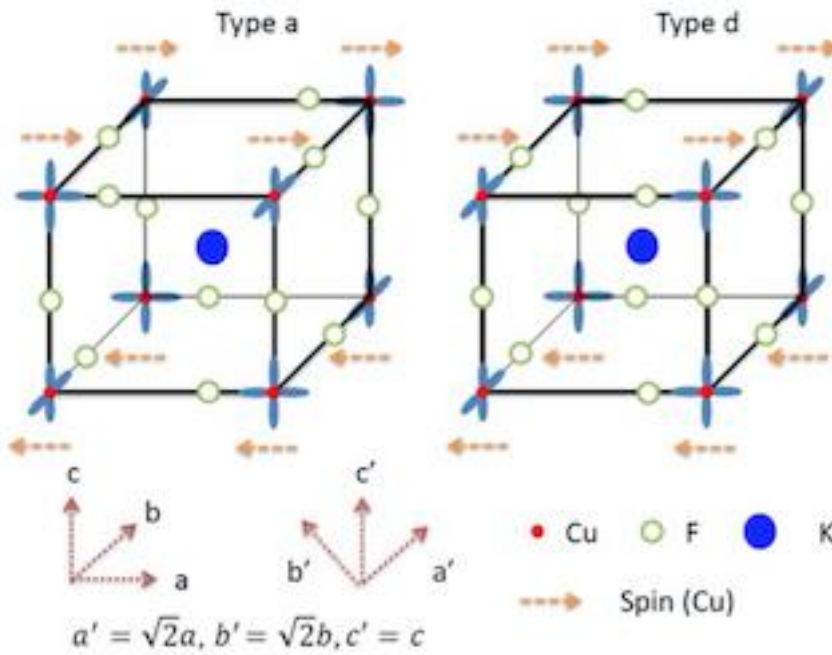


Fig. 1 Schematic views of atomic, spin, and orbital patterns of  $\text{KCuF}_3$ ; antiferro-ordered orbital pattern for *type-a* structure (left) and ferro-ordered orbital pattern for *type-d* structure (right), respectively.

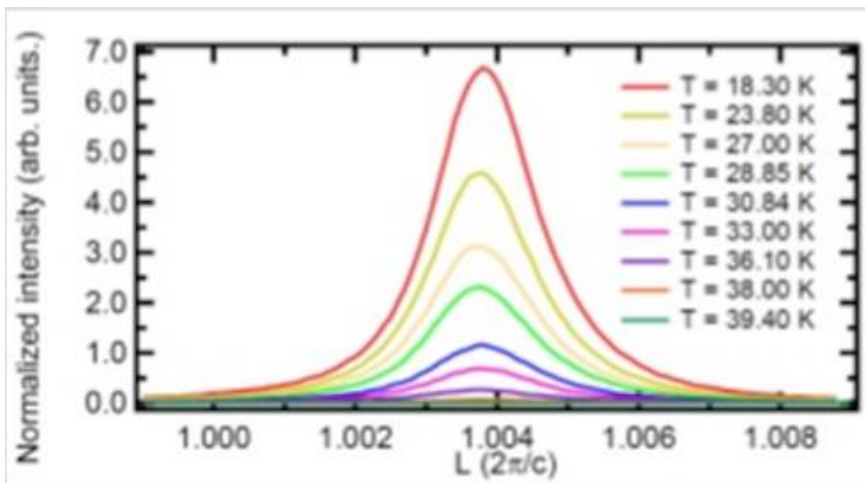


Fig. 2 Momentum scans of resonant soft X-ray scattering of  $\text{KCuF}_3$  for the magnetic reflection  $(0\ 0\ 1)$  along out of plane direction  $[111]$ . The incident photon energy is set at  $\text{Cu } L_3$  edge.

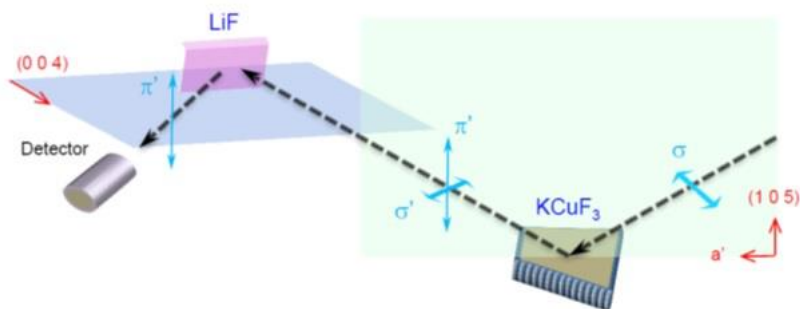


Fig. 3 Schematic illustration of experimental setup for RXS measurement.

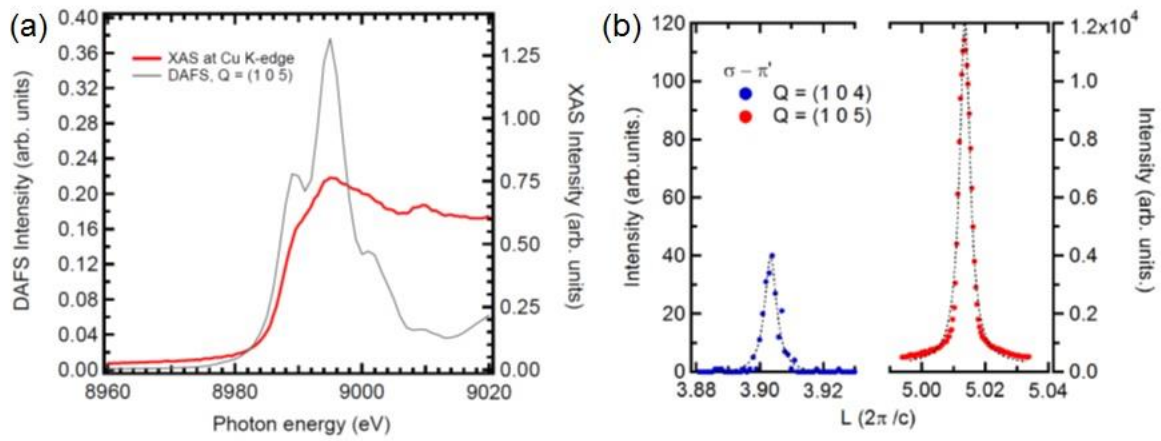


Fig. 4 (a) XAS and integrated intensity of the orbital reflection (1 0 5) spectra of  $\text{KCuF}_3$ . (b) Diffraction peaks of orbital ordering. The blue and red lines are orbital reflections of (1 0 4) for *type-d* and (1 0 5) for *type-a*, respectively.

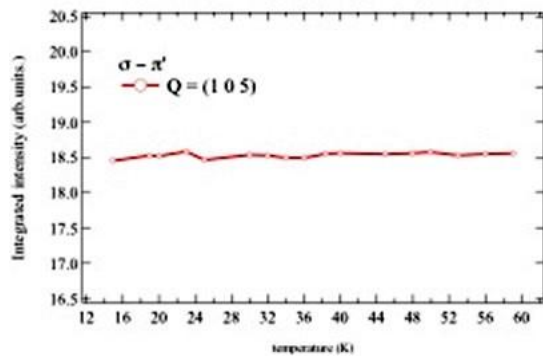


Fig. 5 Temperature dependence of integrated scattering intensity at (1 0 5) in  $\sigma$  (photon-in)- $\pi'$  (photon-out) channel.

©JASRI

(Received: September 30, 2016; Early edition: March 24, 2017;  
Accepted: July 18, 2017; Published: August 17, 2017)